INSTITUT NATIONAL DE RECHERCHE EN INFORMATIQUE ET EN AUTOMATIQUE

A Hybrid Model Based on Continuous Fluctuation Corrections

Maria-Vittoria Salvetti, Hilde Ouvrard, Bruno Koobus, Simone Camarri, Alain Dervieux

N° 6564

18 juin 2008

Thème NUM

Rapport de recherche

ISRN INRIA/RR--6564--FR+ENG

SN 0249-6399

A Hybrid Model Based on Continuous Fluctuation Corrections

Maria-Vittoria Salvetti*, Hilde Ouvrard†, Bruno Koobus‡, Simone Camarri§, Alain Dervieux¶

Thème NUM — Systèmes numériques
Projet Smash

Rapport de recherche n° 6564 — 18 juin 2008 — 21 pages

Abstract: A novel method is proposed for blending RANS and VMS-LES approaches in a hybrid model. To this purpose, the flow variables are decomposed in a RANS part (i.e. the averaged flow field), a correction part that takes into account the turbulent large-scale fluctuations, and a third part made of the unresolved or SGS fluctuations. The basic idea is to solve the RANS equations in the whole computational domain and to correct the obtained averaged flow field by adding, where the grid is adequately refined, the remaining resolved fluctuations. The RANS model is of low-Reynolds K-EPSILON type. To obtain a model which progressively switches from the RANS to the LES mode, a smooth blending function is introduced to damp the correction term. Different definitions of the blending function are proposed and investigated. The capabilities of the proposed hybrid approach are appraised in the simulation of the flow around a circular cylinder at $Re = 140000$. Results are compared to those of other hybrid simulations in the literature and to experimental data.

Key-words: Turbulence, Hybrid RANS/LES approach, bluff-body flows, variational multi-scale, unstructured meshes

* Dipl. Ingegneria Aerospaziale, Via Caruso,56126 Pisa (Italy)
† Dept Mathématiques, Univ. Montpellier II, CC.051, 34095 Montpellier, France
‡ Dept Mathématiques, Univ. Montpellier II, CC.051, 34095 Montpellier, France, and INRIA
§ Dipl. Ingegneria Aerospaziale, Via Caruso,56126 Pisa (Italy)
¶ INRIA, 2004 Route des Lucioles, BP. 93, 06902 Sophia-Antipolis, France

Un modèle hybride par correction continue des fluctuations

Résumé : Ce rapport décrit une nouvelle méthode d'hybridation des modèles RANS et VMS-LES. ans ce but, les variables de l'écoulement sont décomposées en une partie moyenne, une partie de correction correspondant aux fluctuations des grandes échelles résolues et une dernière partie correspondant aux échelles non-résolues. Le principe de cette approche est de résoudre les équations de Navier-Stokes en moyenne de Reynolds sur tout le domaine de calcul et d'ajouter à l'écoulement moyen un terme de correction qui prend en compte les fluctuations résolues lorsque que le maillage est suffisamment fin. Le modèle RANS utilisé est le modèle K-EPSILON, en version bas Reynolds. Un paramètre de couplage θ contrôle l'hybridation progressive de ces modèles. Plusieurs définitions de ce paramètre sont considérées dans ce rapport. Ce modèle est appliqué à la simulation d'un écoulement turbulent autour d'un cylindre circulaire à $Re = 140000$. Les résultats obtenus sont comparés à d'autres résultats numériques et à des résultats expérimentaux.

Mots-clés : Turbulence, Hybride RANS/LES, écoulements autour d'obstacles, Variational Multiscale, maillages non-structurés

1 Introduction

The most widely used approach for the simulation of high-Reynolds number turbulent flows is the one based on the Reynolds-Averaged Navier-Stokes equations (RANS). However, RANS models usually have difficulties in providing accurate predictions for flows with massive separations, as for instance the flow around bluff bodies. An alternative approach is the Large-Eddy simulation (LES), which, for massively separated flows, is generally more accurate, but also computationally more expensive, than RANS. Moreover, the cost of LES simulations increases as the flow Reynolds number is increased. Indeed, the grid has to be fine enough to resolve a significant part of the turbulent scales, and this becomes particularly critical in the near-wall regions. A new class of models has recently been proposed in the literature in which RANS and LES approaches are combined together in order to obtain simulations as accurate as in the LES case but at reasonable computational costs. These hybrid methods can be divided in *zonal* approaches (e.g. [8], [15], [30] and [32]), in which the regions where RANS and LES are used are a-priori defined, and the so called *universal* models, which should be able to automatically switch from RANS to LES throughout the computational domain. In the perspective of the simulation of massively separated unsteady flows in complex geometry, as occur in many cases of engineering or industrial interest, we are primarily interested in universal hybrid models. Among the universal hybrid models described in the literature, the *Detached Eddy Simulation* (DES) has received the largest attention. This approach [28] is generally based on the Spalart-Allmaras RANS model, modified in such a way that, in the near-wall region and with RANS-like grids the Spalart-Allmaras RANS model is used, while far from solid walls and with refined grids, the simulation switches to the LES mode with a one-equation SGS closure. Another universal hybrid approach is the *Limited Numerical Scales* (LNS, [2]), in which the blending parameter depends on the values of the eddy-viscosity given by a RANS model and of the SGS viscosity given by a LES closure. In practice, the minimum of the two eddy-viscosities is used (see also [7] for an example of application of LNS to the simulation of bluff-body flows).

A major difficulty in combining a standard RANS model with a LES one is due to the fact that the RANS equations govern the averaged flow field, while the LES equations describe the evolution of spatially filtered, fluctuating variables. RANS solution can be steady or only contains the unsteadiness of the largest scales, if large-scale unsteadiness is present in the flow (e.g. bluff-body flows). On the other hand, LES needs a significant level of fluctuations in order to model the flow with a sufficient accuracy. This leads to the need of special treatment at the RANS/LES interface regions in zonal approaches (see, e.g., [8], [15], [30] and [32]) and to the so-called *grey-zones* or *modeled stress depletion* ([28] or [2]) for universal models. More generally, finding strategies building universal hybridization models, i.e. able to combine a large class of statistical models with a large class of LES is still an open issue.

In the present work, such a strategy for blending RANS and LES approaches in a hybrid model is proposed. To this purpose, the NLDE (Non-Linear Disturbance Equations) technique is used [17], in which the flow variables are decomposed in a RANS part (i.e. the averaged flow field), a correction part that takes into account the turbulent large-scale fluctuations, and a third part made of the unresolved or SGS fluctuations. The basic idea is to solve the RANS equations in the whole computational domain and to correct the obtained averaged flow field by adding, where the grid is adequately refined, the remaining resolved fluctuations. The NLDE technique was formulated and used as a zonal approach ([17], [31], [30]). In contrast, we search here for a hybridization strategy in which the RANS and LES models are blended in the computational domain following a given criterion. To this aim, a blending function is introduced, θ, which smoothly varies between 0 and 1. The correction term which is added to the averaged flow field is thus damped by a factor $(1-\theta)$, obtaining a model which coincides with the RANS approach when $\theta = 1$ and recovers the LES approach in the limit of $\theta \to 0$. For θ going from 0 to 1, i.e. when the model switches from the RANS to the LES mode, a progressive addition of fluctuations is obtained and is aimed at avoiding, although in an empirical manner, the previously mentioned problems occuring for abrupt switches from RANS to LES (and vice versa). Following strictly these guidelines would imply that the two fields, RANS and LES correction, need to be computed separately. In this first paper, we explore a single field version and investigate several other ingredients of the proposed hybrid family. In particular, three different definitions of the blending function θ are proposed and will be examined in this paper. They are based on the ratios between (i) two eddy viscosities, (ii) two characteristic length scales and (iii) two characteristic time scales given by the RANS and the LES models, respectively. A low-Reynolds version of the $k-\varepsilon$ model [11] is used here as RANS closure, while for the LES part the Variational Multi-Scale approach (VMS) is adopted [13]. Note that the proposed hybridization strategy does not require any particular RANS or LES closure as soon as characteristic length scales or time scales can be defined. It permits a natural integration of the VMS concept, while this is not the case for other existing approaches, as LNS or DES. The VMS approach can be compared in terms of accuracy to the dynamic Smagorinsky model, but its computational cost is definitely lower and comparable to that of the simple Smagorinsky model (see [16]). The extension of VMS to unstructured meshes [16] [26] opens the way for industrial applications.

The capabilities of the proposed hybrid approach, refered in the sequel as the *Fluctuation Correction Model* (FCM), are appraised in the simulation of the flow around a circular cylinder at $Re = 140000$ (based on the far-field velocity and the cylinder diameter). Comparisons with experimental data and DES simulations in the literature are provided. The sensitivity to the blending function definition, to the closure model for the LES part and to grid refinement are investigated.

2 Hybrid RANS/LES coupling

The Navier-Stokes equations for compressible flows of (calorically and thermally) perfect Newtonian gases are considered here, in conservative form and using the following variables: W=(ρ, ρu_i $(i = 1, 2, 3)$, E), where ρ is the density, ρu_i is momentum and E is the total energy per unit volume ($E = \rho e + 1/2 \rho u_i u_i$, e being the internal energy).

As in [17], the following decomposition of the flow variables is adopted:

$$W = \underbrace{< W >}_{RANS} + \underbrace{W^c}_{correction} + W^{SGS}$$

where $< W >$ are the RANS flow variables, obtained by applying an averaging operator to the Navier-Stokes equations, W^c are the remaining resolved fluctuations (i.e. $< W > + W^c$ are the flow variables in LES) and W^{SGS} are the unresolved or SGS fluctuations.

If we write the Navier-Stokes equations in the following compact conservative form:

$$\frac{\partial W}{\partial t} + \nabla \cdot F(W) = 0$$

in which F represents both the viscous and the convective fluxes, for the averaged flow $\langle W \rangle$ we get:

$$\frac{\partial \langle W \rangle}{\partial t} + \nabla \cdot F(\langle W \rangle) = -\tau^{RANS}(\langle W \rangle) \tag{1}$$

where $\tau^{RANS}(\langle W \rangle)$ is the closure term given by a RANS turbulence model.

As well known, by applying a filtering operator to the Navier-Stokes equations, the LES equations are obtained, which can be written as follows:

$$\frac{\partial \langle W \rangle + W^c}{\partial t} + \nabla \cdot F(\langle W \rangle + W^c) = -\tau^{LES}(\langle W \rangle + W^c) \tag{2}$$

where τ^{LES} is the SGS term.

An equation for the resolved fluctuations W^c can thus be derived (see also [17]):

$$\frac{\partial W^c}{\partial t} + \nabla \cdot F(\langle W \rangle + W^c) \; - \; \nabla \cdot F(\langle W \rangle) = \tau^{RANS}(\langle W \rangle) - \tau^{LES}(\langle W \rangle + W^c) \tag{3}$$

The basic idea of the proposed hybrid model is to solve Eq. (1) in the whole domain and to correct the obtained averaged flow by adding the remaining resolved fluctuations (computed through Eq. (3)), wherever the grid resolution is adequate for a LES. To identify the regions where the additional fluctuations must be computed, we introduce a *blending function*, θ, smoothly varying between 0 and 1. When $\theta = 1$, no correction to $\langle W \rangle$ is computed and, thus, the RANS approach is recovered. Conversely, wherever $\theta < 1$, additional resolved fluctuations are computed; in the limit of $\theta \to 0$ we want to recover a full LES approach. The definition of the blending function is discussed in details in Sec. 6. Thus, the following equation is used here for the correction term:

$$\frac{\partial W^c}{\partial t} \; + \; \nabla \cdot F(\langle W \rangle + W^c) \; - \; \nabla \cdot F(\langle W \rangle) = (1-\theta) \left[\tau^{RANS}(\langle W \rangle) - \tau^{LES}(\langle W \rangle + W^c) \right] \tag{4}$$

Note that for $\theta \to 1$ the RANS limit is actually recovered; indeed, for $\theta = 1$ the right-hand side of Eq. (4) vanishes and, hence, a trivial solution is $W^c = 0$. As required, for $\theta = 0$ Eq. (4) becomes identical to Eq. (3) and the remaining resolved fluctuations are added to the averaged flow; the model, thus, works in LES mode. For θ going from 1 to 0, i.e. when, following the definition of the blending function (see Sec. 6), the grid resolution is intermediate between one adequate for RANS and one adequate for LES, the right-hand side term in Eq. (4) is damped through multiplication by $(1-\theta)$. Although it could seem rather arbitrary from a physical point of view, this is aimed to obtain a smooth transition between RANS and LES. More specifically, we wish to obtain a progressive addition of fluctuations when the grid resolution increases and the model switches from the RANS to the LES mode.

Summarizing, the ingredients of the proposed approach are: a RANS closure model, a SGS model for LES and the definition of the blending function. These will be described in Secs. 4, 5 and 6.

3 Basic numerical ingredients

The governing equations are discretized in space using a mixed finite-volume/finite-element method applied to unstructured tetrahedrizations. The adopted scheme is vertex centered, i.e. all degrees of freedom are located at the vertices. P1 Galerkin finite elements are used to discretize the diffusive terms. A dual finite-volume grid is obtained by building a cell C_i around each vertex i. The convective fluxes are discretized in terms of fluxes through the common boundaries shared by neighboring cells. The Roe scheme [22] represents the basic upwind component for the numerical evaluation of the convective fluxes. A Turkel-type preconditioning term is introduced to avoid accuracy problems at low Mach numbers [12]. A parameter γ_s multiplies the upwind part of the scheme and permits a direct control of the numerical viscosity, leading to a full upwind scheme for $\gamma_s = 1$ and to a centered scheme when $\gamma_s = 0$. The resulting numerical approximation of the convective flux between the i-th and the j-th cells is the following:

$$\Phi^R\left(W_i,\ W_j,\ \vec{n}\right) = \frac{\mathcal{F}\left(W_i,\ \vec{n}\right) + \mathcal{F}\left(W_j,\ \vec{n}\right)}{2} - \gamma_s \left[P^{-1}|P\mathcal{R}|\ \frac{W_j - W_i}{2}\right] \tag{5}$$

in which W_i is the solution vector at the i-th node, $\vec{n}$ is the outward normal to the cell boundary and $\mathcal{R}\left(W_i,\ W_j,\ \vec{n}\right)$ is the Roe Matrix. The matrix $P(W_i,\ W_j)$ is the preconditioning term. Note that, since it only appears in the upwind part of the numerical fluxes, the scheme remains consistent in time and can thus be used for unsteady flow simulations. The MUSCL linear reconstruction method ("Monotone Upwind Schemes for Conservation Laws" [34]) is employed to increase the order of accuracy of the Roe scheme. This is obtained by expressing the Roe flux between two cells, centered on two generic nodes i and j, as a function of the reconstructed values of W at their interface. A reconstruction using a combination of different families of approximate gradients is adopted [5], which allows a numerical dissipation made of sixth-order space derivatives, and, thus, concentrated on a narrow-band of the highest resolved frequencies, to be obtained. This is important in LES simulations to limit as far as possible the interactions between numerical and SGS dissipation, which could deteriorate the accuracy of the results.

An implicit time marching algorithm is used, based on a second-order time-accurate backward difference scheme.

More details on the numerical ingredients used in the present work can be found in [5] and [9].

4 RANS closure model

As far the closure of the RANS equations is concerned, the Low Reynolds $k-\varepsilon$ model proposed in [11] is considered. The Reynolds stress tensor has the same form as in the standard $k-\varepsilon$ model but here the turbulent eddy-viscosity μ_t is defined as follows:

$$\mu_t = C_\mu f_\mu \frac{k^2}{\epsilon} \tag{6}$$

where C_μ has the same value as in the standard $k-\varepsilon$ multiplied by a damping function f_μ, chosen as follows:

$$f_\mu = \frac{1-e^{-A_\mu R_t}}{1-e^{-R_t^{1/2}}} max(1, \psi^{-1}) \tag{7}$$

where $\psi = R_t^{1/2}/C_\tau$, $R_t = k^2/(\nu\varepsilon)$ is the turbulent Reynolds number (ν being the kinematic viscosity) and $A_\mu = 0.01$; and k and ε are determined by ad-hoc modeled transport equations (see [11]).

5 Variational Multiscale LES formulation and SGS models

For the LES mode, we wish to recover the Variational Multi-Scale approach [13], in which the flow variables are decomposed as follows:

$$W = \underbrace{\overline{W}}_{LRS} + \underbrace{W'}_{SRS} + W^{SGS} \tag{8}$$

where $\overline{W}$ are the large resolved scales (LRS) and W' are the small resolved scales (SRS). This decomposition is obtained by variational projection in the LRS and SRS spaces respectively. In the present study, we follow the VMS approach proposed in [16] for the simulation of compressible turbulent flows through a finite volume/finite element discretization on unstructured tetrahedral grids. Let χ_l and ϕ_l be the N finite-volume and finite-element basis functions associated to the used grid. In order to obtain the VMS flow decomposition, the finite dimensional spaces $\mathcal{V}_{FV}$ and $\mathcal{V}_{FE}$, respectively spanned by χ_l and ϕ_l, can be in turn decomposed in $\overline{\mathcal{V}}_{FV}$ and $\mathcal{V}'_{FV}$ and in $\overline{\mathcal{V}}_{FE}$ and $\mathcal{V}'_{FE}$ [16], $\overline{\mathcal{V}}_{FV}$ and $\mathcal{V}'_{FV}$ being the finite volume spaces associated to the largest and smallest resolved scales, spanned by the basis functions $\overline{\chi_l}$ and χ_l'; $\overline{\mathcal{V}}_{FE}$ and $\mathcal{V}_{FE}'$ are the finite element analogous. In [16], the basis functions of the LRS space are defined through a projector operator in the LRS space, based on spatial average on macro cells:

$$\overline{\psi}_k = \frac{Vol(C_k)}{\sum_{j\epsilon I_k} Vol(C_j)} \sum_{j\epsilon I_k} \psi_j \tag{9}$$

for finite volumes, and:

$$\overline{\phi}_k = \frac{Vol(C_k)}{\sum_{j\epsilon I_k} Vol(C_j)} \sum_{j\epsilon I_k} \phi_j \tag{10}$$

for the diffusive terms, discretized by finite elements. In both Eqs. (9) and (10), $I_k = \{j/C_j \in C_{m(k)}\}$, $C_{m(k)}$ being the macro-cell containing the cell C_k. The macro-cells are obtained by a process known as agglomeration [18]. The basis functions for the smallest resolved scales (SRS) space are clearly obtained as follows: $\psi_l' = \psi_l - \overline{\psi}_l$ and $\phi_l' = \phi_l - \overline{\phi}_l$.

Finally, a key feature of the VMS approach is that the SGS model is added only to the smallest resolved scales. As in [16], eddy-viscosity models are used here, and, hence, the SGS terms are discretized analogously to the viscous fluxes. Thus, the Galerkin projection of Eq. (2) becomes:

$$\begin{aligned} &\left(\frac{\partial\langle W\rangle + W^c}{\partial t}, \chi_l\right) + (\nabla\cdot F_c(\langle W\rangle + W^c), \chi_l) + \\ &(\nabla\cdot F_v(\langle W\rangle + W^c), \phi_l) = -\left(\ \tau^{LES}(W'), \phi_l'\right) \quad l = 1, N \end{aligned} \tag{11}$$

in which $(\cdot,\cdot)$ denotes the L^2 scalar product.

In this context, the Galerkin projection of Eqs. (1) and (4) for the computation of $\langle W\rangle$ and of the additional fluctuations in the proposed hybrid model become respectively:

$$\begin{aligned} &\left(\frac{\partial\langle W\rangle}{\partial t}, \chi_l\right) + (\nabla\cdot F_c(\langle W\rangle), \chi_l) + (\nabla\cdot F_v(\langle W\rangle), \phi_l) = \\ &-\left(\tau^{RANS}(\langle W\rangle), \phi_l\right) \quad l = 1, N \end{aligned} \tag{12}$$

$$\begin{aligned} &\left(\frac{\partial W^c}{\partial t}, \chi_l\right) + (\nabla\cdot F_c(\langle W\rangle + W^c), \chi_l) - (\nabla\cdot F_c(\langle W\rangle), \chi_l) + \\ &(\nabla\cdot F_v(W^c), \phi_l) = (1-\theta)\left[\left(\ \tau^{RANS}(\langle W\rangle), \phi_l\right) - \left(\tau^{LES}(W'), \phi_l'\right)\right] \quad l = 1, N \end{aligned} \tag{13}$$

As for the closure model for LES, giving the expression of τ^{LES} in Eqs. (12) and (13), three different eddy-viscosity models have been considered. The first one is the Smagorinsky model [27] giving the following expression for the eddy viscosity:

$$\nu_s^{(S)} = (C_s\Delta)^2\sqrt{S_{ij}'S_{ij}'} \tag{14}$$

where C_s is the model input parameter, S'_{ij} is the strain-rate tensor (computed in the VMS approach as a function of W') and Δ is a length which should be representative of the size of the resolved turbulent scales. Here, Δ has been selected as $Vol(i)^{1/3}$ ($Vol(i)$ being the volume of the i-th tetrahedron) and C_s has been set equal to 0.1.

The model proposed by Vreman [35] is also considered, which gives the following expression of the eddy-viscosity:

$$\nu_{\mathrm{s}}^{(V)} = C_V \left(\frac{B_\beta}{\alpha_{ij}\alpha_{ij}}\right)^{\frac{1}{2}} \tag{15}$$

with

$$\alpha_{ij} = \partial u'_j / \partial x_i$$

$$\beta_{ij} = \Delta^2 \alpha_{mi}\alpha_{mj}$$

$$B_\beta = \beta_{11}\beta_{22} - \beta_{12}^2 + \beta_{11}\beta_{33} - \beta_{13}^2 + \beta_{22}\beta_{33} - \beta_{23}^2$$

The constant $C_V \approx 2.5 C_s^2$ where C_s denotes the Smagorinsky constant (see [35]); Δ is the same as for the Smagorinsky model.

The last considered SGS closure is the Wall-Adapting Local Eddy-Viscosity (WALE) SGS model proposed by Nicoud and Ducros [20]. The eddy-viscosity term μ_w in this model is defined by:

$$\nu_{\mathrm{s}}^{(W)} = (C_w \Delta)^2 \frac{({S'_{ij}}^d {S'_{ij}}^d)^{\frac{3}{2}}}{(S'_{ij} S'_{ij})^{\frac{5}{2}} + ({S'_{ij}}^d {S'_{ij}}^d)^{\frac{5}{4}}} \tag{16}$$

with

$${S'_{ij}}^d = \frac{1}{2}({g'_{ij}}^2 + {g'_{ji}}^2) - \frac{1}{3}\delta_{ij}{g'_{kk}}^2$$

being the symmetric part of the tensor ${g'_{ij}}^2 = g'_{ik} g'_{kj}$, where $g'_{ij} = \partial u'_i / \partial x_j$. The constant C_w is set to 0.1.

6 Definition of the blending function and simplified model

As a possible choice for θ, the following function is used in the present study:

$$\theta = F(\xi) = tanh(\xi^2) \tag{17}$$

where ξ is the *blending parameter*, which should indicate whether the grid resolution is fine enough to resolve a significant part of the turbulence fluctuations, i.e. to obtain a LES-like simulation. The choice of the *blending parameter* is clearly a key point for the definition of the present hybrid model. In the present study, different options are proposed and investigated, namely: the ratio between the eddy viscosities given by the LES and the RANS closures, $\xi_{VR} = \mu_s / \mu_t$, which is also used as a blending parameter in LNS Ref. [2], $\xi_{LR} = \Delta / l_{RANS}$, l_{RANS} being a typical length in the RANS approach, i.e. $l_{RANS} = k^{3/2}\epsilon^{-1}$ and, finally, $\xi_{TR} = t_{LES}/t_{RANS}$, t_{LES} and t_{RANS} being characteristic times of the LES and RANS approaches respectively, $t_{LES} = (S_{ij}S_{ij})^{-1/2}$ and $t_{RANS} = k\epsilon^{-1}$.

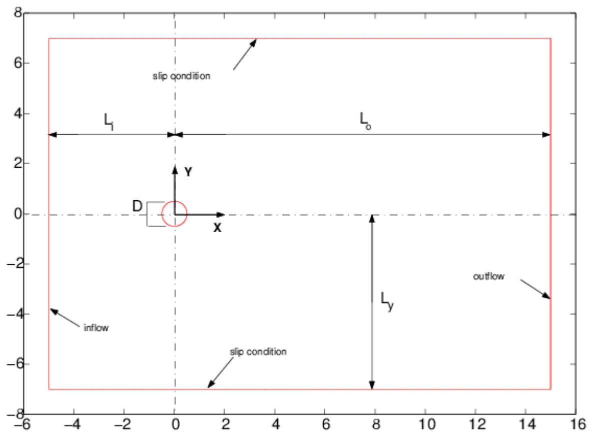

Figure 1: Computational domain

To avoid the solution of two different systems of PDEs and the consequent increase of required computational resources, Eqs. (12) and (13) can be recast together as:

$$\begin{aligned}&\left(\frac{\partial W}{\partial t},\chi_l\right)+\left(\nabla\cdot F_c(W),\chi_l\right)+\left(\nabla\cdot F_v(W),\phi_l\right)=\\&-\theta\left(\,\tau^{RANS}(\langle W\rangle),\phi_l\right)-(1-\theta)\left(\tau^{LES}(W'),\phi_l'\right)\quad l=1,N\end{aligned}\tag{18}$$

Clearly, if only Eq. (18) is solved, $\langle W\rangle$ is not available at each time step. Two different options are possible: either to use an approximation of $\langle W\rangle$ obtained by averaging and smoothing of W, in the spirit of VMS, or to simply use in Eq. (18) $\tau^{RANS}(W)$. Relaying on the well known and previously discussed tendency of RANS model of naturally damping the fluctuations, the second option is adopted here as a first approximation.

7 Hybrid simulations of the flow around a circular cylinder

The proposed approach has been applied to the simulation of the flow around a circular cylinder at $Re = 140000$ (based on the far-field velocity and the cylinder diameter, D). With reference to Fig. 1, the domain dimensions are $L_i/D = 5$, $L_o/D = 15$, $L_y/D = 7$ and $L_z/D = 2$, L_z being the domain size in the spanwise direction. On the side surfaces free-slip is imposed and the flow is assumed to be periodic in the spanwise direction. Approximate boundary conditions based on the Reichardt wall-law are used on the cylinder surface (see [6] and [4]). Boundary conditions based on Steger-Warming decomposition [29] are used at the inflow and at the outflow surfaces. The inflow conditions are the same as in the DES simulations of [33]. In particular, the flow is assumed to be highly turbulent by setting the inflow value of eddy-viscosity to about 5 times the molecular viscosity as in the DES simulation of [33]. This setting corresponds to a free-stream turbulence level $Tu = \overline{u'^2}/U_0$ (where u' is the inlet fluctuation velocity and U_0 is the free-stream mean velocity) of the order of 4%. As discussed also in [33], the effect of such a high level of free-stream turbulence is to make the boundary layer almost entirely turbulent also at the relatively moderate considered Reynolds number and this allows the proposed hybridization strategy to be tested in a case in which it should actually work in RANS mode in the whole boundary layer.

Two different grids are considered; the first one (GR1) has $4.6{\times}10^5$ nodes, while the second one has (GR2) $1.4{\times}10^6$ nodes. The main characteristics of the grids are summarized in Tab. 1. Both grids are composed of a structured part in a circular crown around the

Grid	Elements	Nodes	N_θ	N_z	N_r	t/D
GR1	2.6 10^6	4.6 10^5	180	40	25	0.1
GR2	8.1 10^6	1.4 10^6	360	80	13	0.05

Table 1: Main characteristics of the computational grids. N_θ is the number of nodes over the cylinder in the azimuthal direction, N_z is the number of nodes in the spanwise direction, N_r is the number of nodes in the radial direction inside the crown of thickness t around the cylinder.

cylinder boundary (see Figs. 2) and a unstructured part in the rest of the domain. Inside the structured zone, the nodes are uniformely distributed in the azimuthal and spanwise directions, with the refined grid GR2 having a number of nodes in each direction twice the one in GR1. On the other hand, the radial distribution of nodes inside the structured zone is logarithmic and the resolution is the same for both grids, with a distance of the nearest point to the cylinder boundary of $0.004D$ which corresponds to $y^+ \approx 28$. Note that, to limit the total number of nodes, for GR2 the radial thickness of the structured crown is half of that for GR1.

The main parameters characterizing the simulations carried out with the FCM are summarized in Tab. 2. The numerical method is the one briefly described in Sec. 3. The RANS

Simulation	Blending parameter	Grid	SGS model
FCM1	Viscosity ratio	GR1	Smagorinsky
FCM2	Length ratio	GR1	Smagorinsky
FCM3	Length ratio	GR2	Smagorinsky
FCM4	Length ratio	GR1	Vreman
FCM5	Length ratio	GR1	Wale

Table 2: Main characteristics of the hybrid RANS/VMS-LES simulations

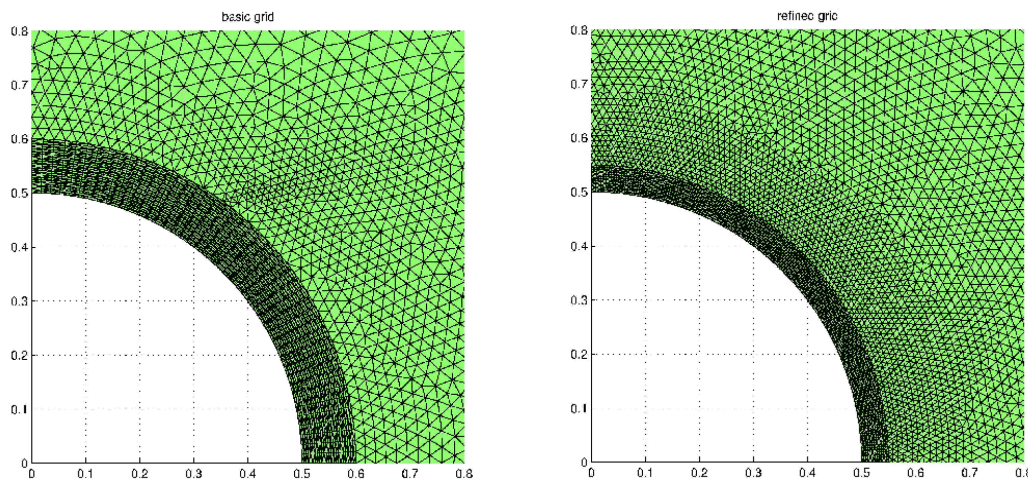

(a) (b)

Figure 2: Zoom of the computational grids near the cylinder in the plane $z = 0$; (a) GR1, (b) GR2.

model is the Low-Reynolds $k-\varepsilon$ model briefly described in Sec. 4. The LES closure is based on the VMS approach (see Sec. 5). Different SGS models are used in the simulations, and namely those described in Sec. 5. Moreover, the sensitivity to the definition of the blending parameter has been investigated.

The maximum time step used in the simulations is set in order to have at least 1500 time steps per shedding cycle and the statistics are obtained by averaging in the spanwise direction and in time over at least 20 shedding cycles. The convergence of the statistics has been checked.

The main flow bulk parameters obtained in the present simulations are summarized in Tab. 3, together with the results of DES simulations in the literature and some experimental data. The results obtained in a 3D unsteady RANS simulation carried out with the Low-Reynolds $k - \varepsilon$ model on the GR1 grid are also reported. We did not carry out a LES simulation, due to the difficulty in imposing in LES the highly turbulent inflow conditions. However, based on previous studies in the literature (see e.g. [3]), it can be inferred that the used grids are plausibly too coarse to obtain satisfactory results in LES at this Reynolds number.

As a general consideration, the agreement with the DES results is fairly good for all the simulations carried out with the FCM approach. As for the comparison with the experiments, as also stated in Travin et al. [33], since our simulations are characterized by a high level of turbulence intensity at the inflow, it makes sense to compare the results

Simulations	Re	$\overline{C_d}$	C_l'	St	l_r	$-C_{pb}$
FCM1	1.4 10^5	0.62	0.083	0.30	1.20	0.72
FCM2	1.4 10^5	0.62	0.083	0.30	1.19	0.65
FCM3	1.4 10^5	0.54	0.065	0.33	1.13	0.63
FCM4	1.4 10^5	0.65	0.077	0.28	1.14	0.72
FCM5	1.4 10^5	0.66	0.094	0.28	1.24	0.72
RANS	1.4 10^5	0.756	0.433	0.275	0.67	0.85
DES [33]	1.4 10^5	0.57-0.65	0.06-0.1	0.28-0.31	1.1 -1.4	0.65-0.7
DES [19]	1.4 10^5	0.6-0.81	–	0.29-0.3	0.6-0.81	0.85-0.91
Exp. [14]	3.8 10^6	0.58	–	0.25	–	0.58
Exp. [1]	5 10^6	0.7	–	–	–	–
Exp. [23]	8.4 10^6	0.7	–	0.27	–	0.8
Exp. [25]	8 10^6	0.52	0.06	0.28	–	–

Table 3: Main bulk flow quantities for the circular cylinder test case. $\overline{C_d}$ is the mean drag coefficient, C_l' is the r.m.s. of the lift coefficient, St the vortex shedding frequency made nondimensional by the cylinder diameter and the freestream velocity, l_r is the length of the mean recirculation bubble and C_{pb} the value of the mean pressure coefficient in the separated wake.

with experiments at higher Reynolds number, in which, although the level of turbulence intensity of the incoming flow is very low, the transition to turbulence of the boundary layer occurs upstream separation. The agreement with these high Re experiments is indeed fairly good, as shown in Tab. 3 and in Figs. 3, showing the distribution of the mean pressure coefficient over the cylinder surface. Conversely, the results of the RANS simulation show significant discrepancies with respect to the DES and the experimental data and, namely, a noticeably higher absolute value of the C_p in the wake, which results in an overestimated mean drag coefficient. Moreover, the mean recirculation bubble is significantly shorter than in the reference experiments and in the hybrid simulations, and this is connected with an overestimation of the amplitude of lift oscillations (see the values of C_l' in Tab. 3). An example of the time behavior of the lift coefficient for a hybrid simulation (FCM2) is given in Fig. 4a and can be compared with the one obtained in the unsteady RANS simulation shown in Fig. 4b. Besides the larger amplitude of the C_l oscillations, it is evident that in the RANS simulation the modulations of the amplitude of these oscillations are significantly less important than in the hybrid simulations. Since such modulations are due to 3D effects in the wake, this is related to the known tendency of the RANS approach to damp 3D phenomena due to the too large introduced turbulent viscosity. This is confirmed also by the instantaneous field values of the spanwise velocity and of the vorticity components ω_x and ω_y, which are much lower in the RANS simulation than in the hybrid ones (not shown here for sake of brevity).

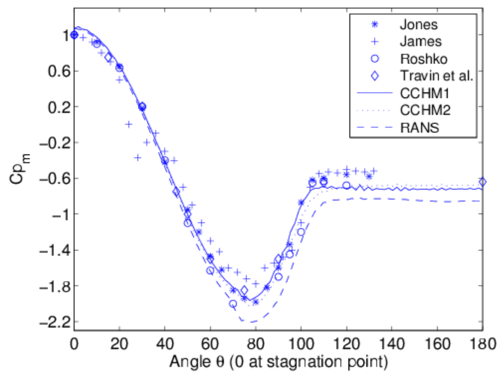

(a)

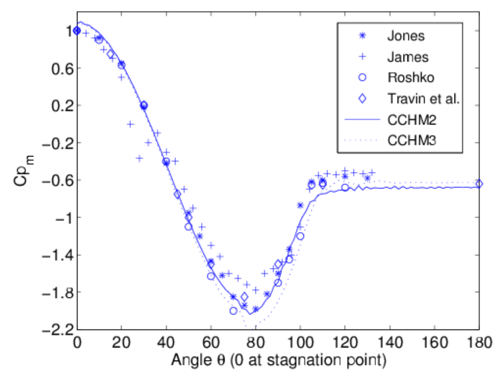

(b)

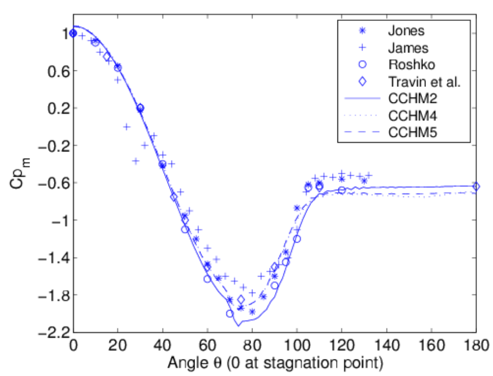

(c)

Figure 3: Distribution over the cylinder surface of the mean pressure coefficient obtained in the different simulations compared to experimental data and to DES results. Different sets of simulations are shown in different panels.

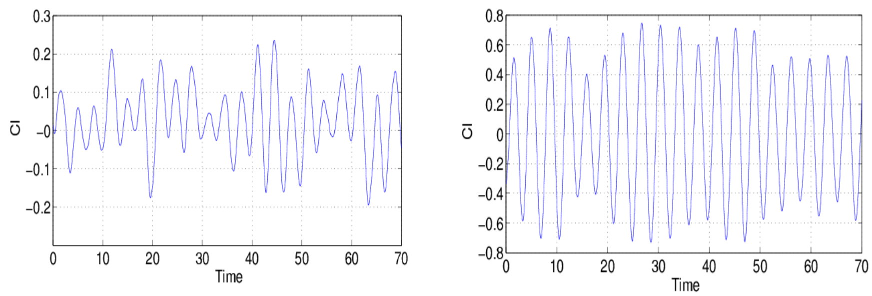

(a) (b)

Figure 4: Time variation of the lift coefficient. (a) FCM2 hybrid simulation; (b) unsteady RANS simulation.

As for the behavior of the hybridization strategy in the field, for all the definitions of the blending parameter, the model actually works in RANS mode in the boundary layer and in the shear-layers detaching from the cylinder, while in the wake a full LES correction is recovered. This is shown, for instance, in Fig. 5, in which the instantaneous isocontours of spanwise vorticity obtained in the simulation FCM2 are reported, to which the isolines of the blending function $\theta = 0.1$ and $\theta = 0.9$ are superimposed. This a-posteriori confirms that the introduced blending function is actually able to give, at least qualitatively, the desired behavior in hybrid simulations of bluff-body flows, without any need of imposing it a priori. Note that there is a thin layer around the cylinder wake in which the model works in a hybrid way, i.e. damped fluctuations are added. From Fig. 6a it appears that a smooth passage from a RANS modeling in the boundary layer and in the detaching shear-layers to a LES one in the wake is obtained, consistently with one of the aims of the proposed hybridization strategy. This corresponds to a progressive addition of fluctuations, as shown in Fig. 7a, in which the isocontours of the mean resolved fluctuating kinetic energy obtained in the FCM2 simulation are reported.

Figs. 8 show instantaneous fields of the SGS viscosity (μ_s) and RANS viscosity (μ_t) for the FCM2 simulation. These plots confirm the behaviour of the hybrid model in the wake. Indeed, μ_s is lower than μ_t and, since the model works in LES mode, the turbulence fluctuations and the flow unsteadiness are less damped than with the RANS model.

Let us analyze now the sensitivity of the results obtained in the FCM simulations to different parameters and, first, the sensitivity to the definition of the blending parameter, by comparing the results of the simulations FCM1 and FCM2. From Tab. 3, it appears that the results are practically insensitive to the definition of the blending parameter. This is also confirmed, for instance, by the distribution over the cylinder of the mean pressure coefficient, C_p, reported in Fig. 3a. As for the behavior of hybridization strategy, it is also similar for the two definitions of the blending parameter. Analogous results were also found

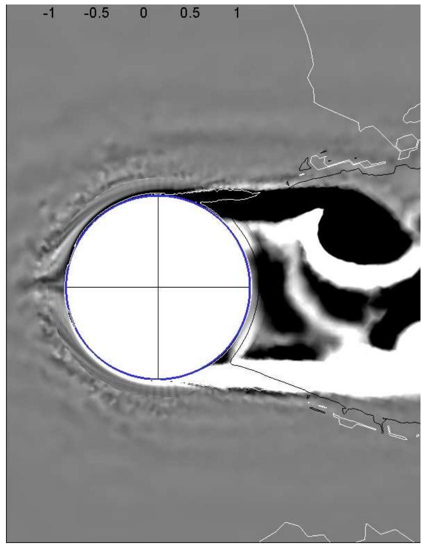

Figure 5: Instantaneous isocontours of spanwise vorticity (simulation FCM2). The isocontours go from the adimensionalized value of -1 (black) to 1 (white). The black and white lines are the isolines of the blending function $\theta = 0.1$ and $\theta = 0.9$.

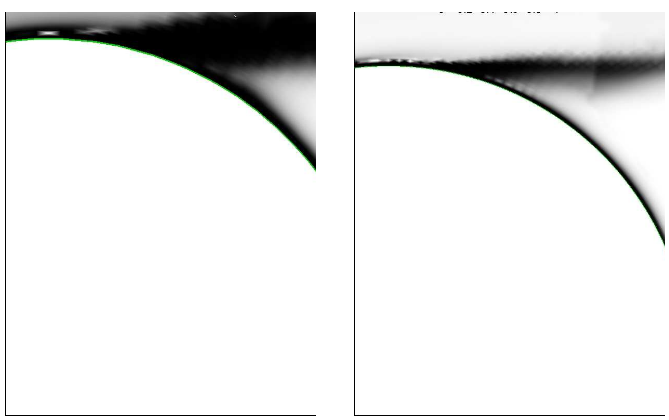

(a) (b)

Figure 6: Instantaneous isocontours of the blending function θ. The isocontours go from 0 (white), corresponding to a full LES correction, to 1 (black), corresponding to pure RANS. Simulations FCM2 (a) and FCM3 (b).

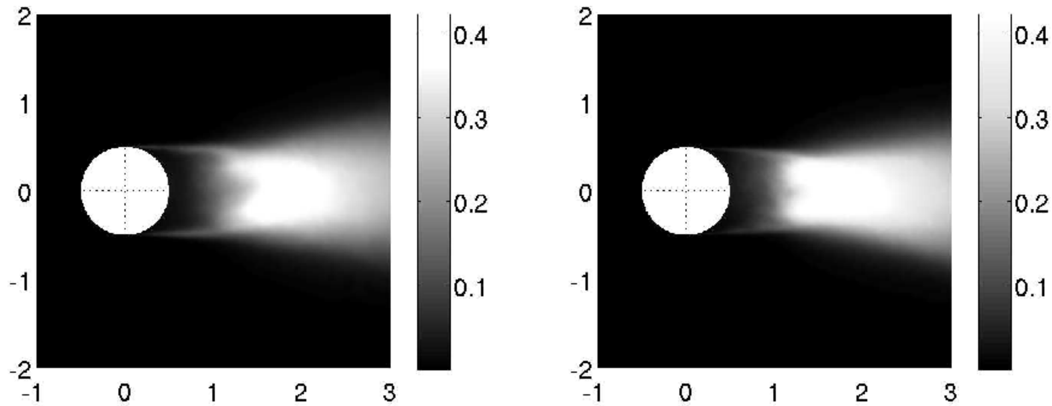

(a) (b)

Figure 7: Isocontours of the resolved fluctuating kinetic energy, averaged in time and in the spanwise direction. Simulations FCM2 (a) and FCM3 (b).

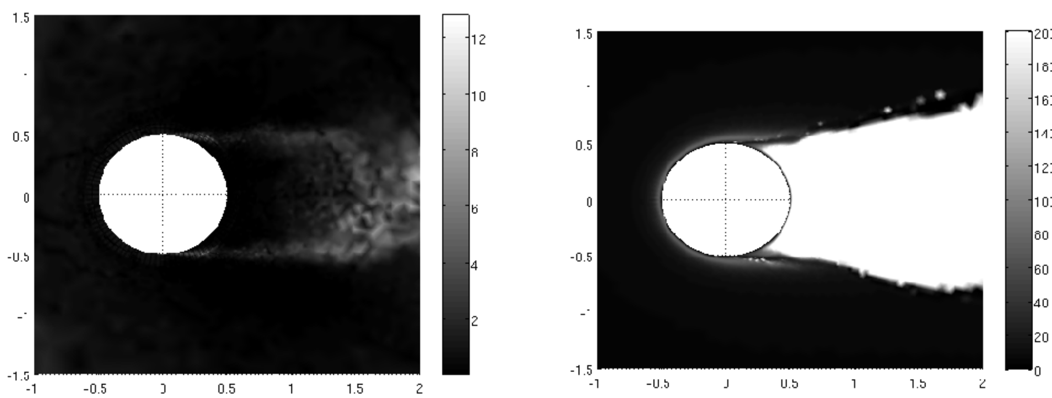

(a) (b)

Figure 8: Instantaneous fields of the SGS viscosity μ_s (a) and the RANS viscosity μ_t (b) for the FCM2 simulation.

with the definition based on the ratio of characteristic times and they are not shown here for sake of brevity. A very low sensitivity of the results to the definition of the blending parameter was also found in the FCM simulations of the flow around a square cylinder described in [10] and [24].

As for the effect of grid refinement, from Tab. 3 it can be seen that it leads to a decrease of $\bar{C}_d$ (compare FCM2 and FCM3). This is due to a decrease of the absolute value of the pressure coefficient in the separated wake (see Tab. 3 and Fig. 3b). However, note that, as it is quite a usual situation for unstructured grids, the refinement carried out to obtain grid GR2 has significantly changed the local quality of the grid (in terms of homogeneity and regularity of the elements) and this may enhance the sensitivity of the results. As for the behavior of the hybridization strategy with grid refinement, it is, at least qualitatively, correct. Indeed, the extension of the zone in the detaching shear-layers in which the model works in RANS mode decreases with grid refinement, as shown for instance in Figs. 6, reporting a zoom near the cylinder of the instantaneous isocontours of the blending function θ, obtained in the simulations FCM2 and FCM3. Furthermore, Fig. 7b shows that, as expected with grid refinement and with the reduced extent of the RANS zone, the regions where the amount of the mean resolved fluctuating kinetic energy starts to become significantly larger are different. With the finer grid, this event happens closer to the cylinder than in the simulation on the coarse grid (FCM2 in Fig. 7a).

Finally, the sensitivity to the SGS model is also very low (compare FCM2, FCM4 and FCM5 in Tab. 3 and Fig. 3c). This very low sensitivity has been observed also in VMS-LES simulations of the same flow carried out at low Reynolds number (see [21]) and, thus, it seems more peculiar to the VMS-LES approach rather than to the hybrid model.

8 Concluding remarks

A strategy for blending RANS and LES has been proposed, which is based on a decomposition of the flow variables in a RANS part and a correction part, which takes into account the resolved fluctuations. The zones in which the correction must be computed and added to the RANS part are not a priori specified, but a blending function is introduced, in order to automatically switch from RANS to LES and vice versa. This function is such that the model works in RANS mode where, based on some criterion, the grid is considered too coarse for LES and tends with continuity to LES as the grid refinement becomes adequate. For complex geometries and complex grid topologies, as e.g. for unstructured grids, this automatic switch may be advantageous with respect to zonal approaches or to methods which requires the definition of the distance from the wall, as DES. Another positive feature is that the proposed strategy does not require any specific RANS or LES closure. In particular, in the present paper, the VMS approach has been integrated in the proposed hybridization strategy for the closure of the LES part, with different eddy-viscosity subgrid scale models. As a first choice, we use here a simplified version of the model, in which only one set of unknowns is computed.

The proposed method has been applied to the hybrid simulations of the flow around a circular cylinder at Re=140000. As in the DES simulations in [33], high turbulence level was assumed at the inflow, in order to have a turbulent boundary layer before separation.

The sensitivity to different parameters, viz. the grid resolution, the SGS model and the definition of the blending parameter, has also been investigated. Unstructured meshes allow for refinement which significantly change the local quality of the grid in terms of homogeneity and regularity of the elements. In that case, results are fairly sensitive to grid resolution and attention need be paid to this effect. The sensitivity to the SGS model in the LES closure is very low. This was also observed (see [21]) for non-hybrid VMS-LES simulations and may be a peculiar feature of the VMS-LES approach rather than of the proposed hybrid approach. The definition of the blending parameter is the most empirical step of the proposed hybridization strategy. Then it is an interesting and positive output of this study that the results are practically insensitive to the definition of the blending parameter, as far as it is chosen among the three options proposed. The behavior of the new method is sound. The blending function, fulfills its role in detecting subregions of the field. The model works in RANS mode in the boundary layer and in the shear layers detaching from the cylinder while complete LES fluctuations are added in the wake, passing through a layer in which the model works in hybrid way, i.e. damped fluctuations are introduced. The quality of prediction is promising. It is in in good agreement with experimental data and compares well to DES simulations in the literature.

References

[1] E. Achenbach. Distribution of local pressure and skin friction around a circular cylinder in cross-flow up to Re= 5×10^6. *J. Fluid Mech.*, 34(4):625–639, 1968.

[2] P. Batten, U. Goldberg, and S. Chakravarthy. Interfacing statistical turbulence closures with large-eddy simulation. *AIAA Journal*, 42(3):485–492, 2004.

[3] M. Breuer. A challenging test case for large eddy simulation: high reynolds number circular cylinder flow. *Int. J. Heat Fluid Flow*, 21(5):648–654, 2000.

[4] S. Camarri and M. V. Salvetti. On the approximate treatment of wall boundary conditions in large-eddy simulation. Technical Report ADIA 2002-3, Dep. Aerospace Engineering - University of Pisa, December 2002.

[5] S. Camarri, M. V. Salvetti, B. Koobus, and A. Dervieux. A low diffusion MUSCL scheme for LES on unstructured grids. *Computers and Fluids*, 33:1101–1129, 2004.

[6] S. Camarri, M.V. Salvetti, B. Koobus, and A. Dervieux. Large-eddy simulation of a bluff-body flow on unstructured grids. *Int. J. Num. Meth. Fluids*, 40:1431–1460, 2002.

[7] S. Camarri, M.V. Salvetti, B. Koobus, and A. Dervieux. Hybrid RANS/LES simulations of a bluff-body flow. *Wind & Structures*, 8:407–426, 2005.

[8] L. Davidson and M. Billson. Hybrid LES-RANS using synthesized turbulent fluctuations for forcing in the interface region. *Int. J. Heat Fluid Flow*, 27:1028–1042, 2006.

[9] C. Farhat, B. Koobus, and H. Tran. Simulation of vortex shedding dominated flows past rigid and flexible structures. In *Computational Methods for Fluid-Structure Interaction*, pages 1–30. Tapir, 1999.

[10] Pagano G., Camarri S., Salvetti M.V., Koobus B., and Dervieux A. Strategies for RANS/VMS-LES coupling. Technical Report RR-5954, INRIA, 2006.

[11] U. Goldberg, O. Peroomian, and S. Chakravarthy. A wall-distance-free $k-\varepsilon$ model with enhanced near-wall treatment. *Journal of Fluids Engineering*, 120:457–462, 1998.

[12] H. Guillard and C. Viozat. On the behaviour of upwind schemes in the low Mach number limit. *Computers and Fluids*, 28:63–86, 1999.

[13] T.J.R. Hughes, L. Mazzei, and K.E. Jansen. Large eddy simulation and the variational multiscale method. *Comput. Vis. Sci.*, 3:47–59, 2000.

[14] W.D. James, S.W. Paris, and G.V. Malcolm. Study of viscous cross flow effects on circular cylinders at high Reynolds numbers. *AIAA Journal*, 18:1066–1072, 1980.

[15] A. Keating, G. De Prisco, and U. Piomelli. Interface conditions for hybrid RANS/LES calculations. *Int. J. Heat Fluid Flow*, 27:777–788, 2006.

[16] B. Koobus and C. Farhat. A variational multiscale method for the large eddy simulation of compressible turbulent flows on unstructured meshes-application to vortex shedding. *Comput. Methods Appl. Mech. Eng.*, 193:1367–1383, 2004.

[17] E. Labourasse and P. Sagaut. Reconstruction of turbulent fluctuations using a hybrid RANS/LES approach. *J. Comp. Phys.*, 182:301–336, 2002.

[18] M.H. Lallemand, H. Steve, and A. Dervieux. Unstructured multigridding by volume agglomeration: current status. *Comput. Fluids*, 21:397–433, 1992.

[19] S.-C. Lo, K.A. Hofmann, and J.-F. Dietiker. Numerical investigation of high Reynolds number flows over square and circular cylinder. *Journal of Thermophysics and Heat Transfer*, 19:72–80, 2005.

[20] F. Nicoud and F. Ducros. Subgrid-scale stress modelling based on the square of the velocity gradient tensor. *Flow Turbulence and Combustion*, 62(3):183–200, 1999.

[21] H. Ouvrard, S. Wornom, B. Koobus, M.V. Salvetti, S. Camarri, and A. Dervieux. Computation of complex unsteady flows around bluff bodies through vms-les modeling. In *Proceedings of West-East High Speed Flow Field Conference*, November 2007.

[22] P.L. Roe. Approximate Riemann solvers, parameters, vectors and difference schemes. *J. Comp. Phys.*, 43:357–372, 1981.

[23] A. Roshko. Pressures and forces on a circular cylinder in cross flow at high reynolds numbers. *J. Fluid. Mech.*, 10:345–356, 1961.

[24] M. V. Salvetti, B. Koobus, H. Ouvrard, S. Camarri, and A. Dervieux. A hybrid model combining RANS and variational multiscale LES. In *IUTAM Symposium on Unsteady Separated Flows and their Control*, 2007.

[25] J.W. Schewe. On the forces acting on a circular cylinder in cross flow from subcritical up to transcritical Reynolds numbers. *J. Fluid Mech.*, 133:265–285, 1983.

[26] S. Sirnivas, S. Wornom, A. Dervieux, B. Koobus, and O. Allain. A study of LES models for the simulation of a turbulent flow around a truss spar geometry. In *Proceedings of OMAE'06, 25^{rd} International Conference on Offshore and Arctic Engineering*, number OMAE2006-92355, Hamburg, Germany, 2006.

[27] J. Smagorinsky. General circulation experiments with the primitive equations. *Monthly Weather Review*, 91(3):99–164, 1963.

[28] P.R. Spalart, W.H. Jou, M. Strelets, and S. Allmaras. *Advances in* DNS/LES, chapter Comments on the feasibility of LES for wings and on a hybrid RANS/LES approach. Columbus (OH), 1997.

[29] J.L. Steger and R.F. Warming. Flux vector splitting for the inviscid gas dynamic equations with applications to the finite difference methods. *J. Comp. Phys*, 40(2):263–293, 1981.

[30] M. Terracol. A zonal RANS/LES approach for noise sources prediction. *Flow Turb. Combustion*, 77:161–184, 2006.

[31] M. Terracol, E. Manoha, C. Herrero, E. Labourasse, S. Redonnet, and P. Sagaut. Hybrid methods for airframe noise numerical predictions. *Theor. Comput. Fluid Dyn.*, 19(3):197–227, 2005.

[32] F. Tessicini, L. Temmerman, and M.A. Leschziner. Approximate near-wall treatments based on zonal and hybrid RANS-LES methods for LES at high Reynolds numbers. *Int. J. Heat Fluid Flow*, 27:789–799, 2006.

[33] A. Travin, M. Shur, M. Strelets, and P. Spalart. Detached-eddy simulations past a circular cylinder. *Flow, Turbulence and Combustion*, 63:293–313, 1999.

[34] B. van Leer. Towards the ultimate conservative scheme. IV: A new approach to numerical convection. *J. Comp. Phys.*, 23:276–299, 1977.

[35] A.W. Vreman. An eddy-viscosity subgrid-scale model for turbulent shear flow: algebraic theory and application. *Physics of Fluids*, 16:3670–3681, 2004.

Unité de recherche INRIA Sophia Antipolis
2004, route des Lucioles - BP 93 - 06902 Sophia Antipolis Cedex (France)

Unité de recherche INRIA Futurs : Parc Club Orsay Université - ZAC des Vignes
4, rue Jacques Monod - 91893 ORSAY Cedex (France)
Unité de recherche INRIA Lorraine : LORIA, Technopôle de Nancy-Brabois - Campus scientifique
615, rue du Jardin Botanique - BP 101 - 54602 Villers-lès-Nancy Cedex (France)
Unité de recherche INRIA Rennes : IRISA, Campus universitaire de Beaulieu - 35042 Rennes Cedex (France)
Unité de recherche INRIA Rhône-Alpes : 655, avenue de l'Europe - 38334 Montbonnot Saint-Ismier (France)
Unité de recherche INRIA Rocquencourt : Domaine de Voluceau - Rocquencourt - BP 105 - 78153 Le Chesnay Cedex (France)

Éditeur
INRIA - Domaine de Voluceau - Rocquencourt, BP 105 - 78153 Le Chesnay Cedex (France)
http://www.inria.fr
ISSN 0249-6399